Desalination and Water Treatment
www.deswater.com

doi: 10.5004/dwt.2017.20139

62 (2017) 11–21
February

Robust design and operation of MSF water desalination process using loop-shaping control procedure

Bui Duc Hong Phuc[a], Sam-Sang You[b,*], Tae-Woo Lim[c], Seok-Kwon Jeong[d]

[a]*Department of Convergence Study on the Ocean Science and Technology, Korea Maritime and Ocean University, Busan, Korea, 606-791, Tel. +82 51 4104360; email: buiduchongphuc@kmou.ac.kr*
[b]*Division of Mechanical Engineering, Korea Maritime and Ocean University, Busan, Korea, 606-791, Tel. +82 51 4104366; email: ssyou@kmou.ac.kr*
[c]*Division of Marine Engineering, Korea Maritime and Ocean University, Busan, Korea, 606-791, Tel. +82 51 4104256; email: kyunlim@kmou.ac.kr*
[d]*Department of Refrigeration and Air-conditioning Engineering, Pukyong National University, Busan, Korea, 608-739, Tel. +82 51 6296181; email: skjeong@pknu.ac.kr*

Received 7 April 2016; Accepted 27 July 2016

ABSTRACT

This paper presents a two-degree-of-freedom (2-DOF) robust (H_∞) loop-shaping algorithm to control and stabilize a multi-stage flash (MSF) desalination plant under parametric uncertainties, external disturbances and measurement noises. In this paradigm, the general uncertainty model represented by coprime factor uncertainty (CFU) description is able to cover both unmodeled dynamics and physical parameter variations at all frequencies. By using 2-DOF H_∞ loop-shaping technique, the designers can shape the frequency response of the original model into the desired shape which satisfies both transient response and robustness against various uncertainties. Top brine temperature and recycle brine flow rate have been chosen to stand for MSF plant performance. The simulation results demonstrate that the achieved controller has high stability margin, excellent abilities of disturbances and noises attenuations. In fact, it can deal with approximately 60% of parameter variations, reject at least 84% of exogenous disturbances, and 80% of sensor noises. Note that most currently used controllers reported cannot cope with those high levels of plant uncertainties and disturbances. Thus, it is necessary to implement the advanced control schemes for effectively controlling MSF plants, ensuring high water quality and optimizing water monitoring system. Finally, this robust control method with reduced-order can help prevent machine faults, stabilize MSF plants, optimize energy usage, and lower water production costs, with overcoming various limitations of some conventional controllers.

Keywords: Coprime factor uncertainty; H_∞ loop-shaping; Multi-stage flash (MSF) desalination; Robust control; Reduced-order controller; Energy-efficient method; Water quality

1. Introduction

Freshwater scarcity is already showing grave problems for arid countries, mostly in Africa, Middle East, and Caribbean regions. As the populations continuously grow, water supplies will become increasingly insufficient. Oceans, which cover more than 70% of the earth's surface and contain 97% of the earth's water, have salt water [1]. The salinity of seawater must be reduced before it can be used. Water desalination is one of the main methods to solve acute water shortage problems. It is known that the two major desalination methods are MSF and reverse osmosis (RO). Before the 1980s, MSF plants had contributed most of the world desalted water. However, during the period 1980–1999, the RO process started to gain ground in the desalination market through progress and development of permeating

* Corresponding author.

membranes with high fluxes, operating at relatively low pressures [2]. Nowadays, although RO process is leading in the global water market, MSF still plays a significant role in desalination industry. Actually, it is the most mature and reliable desalination process since the 1960s. MSF plants are also the dominant type of water desalination in some countries such as Saudi Arabia, Kuwait [3] and the United Arab Emirates.

MSF desalination is a very complex process that consumes a substantial amount of thermal energy [4]. Moreover, its performance is affected by some external factors such as salt concentration and seawater temperature. Therefore, MSF plants need more accurate control systems to maintain their operations in optimum conditions ensuring low product costs without system failures. Many control strategies for automatically manipulating MSF plants have been introduced in the literature. As summarized by Alatiqi et al. [2], the conventional strategies include manual, PID, ratio, cascade and feed-forward approaches. Advanced control methods include gain scheduling, time-delay compensation, decoupling control, dead-time compensation, and Smith-predictor. Other widely used advanced control techniques include model predictive, statistical quality, internal model, adaptive, pattern recognition, and state estimation schemes. New advanced control methods include optimal, nonlinear, expert system, fuzzy, and simulators. However, due to global climate change and higher water demand, plant operators always look for automatic controllers that can lower product costs while coping with increasing external disturbances in MSF plants. Some robust controllers have been designed for MSF systems such as model predictive controller (MPC) [5] and constraint model predictive control [6] but the allowed modeling mismatches are relatively low and there exist some weaknesses in tuning and computational time. Furthermore, external disturbances and noises are not sufficiently considered in the operations of MSF desalination plants so far.

In this paper, a new robust controller using loop-shaping procedure is designed for a specified MSF plant to monitor the water quality under parametric uncertainties, measurement noises, and external disturbances. The ultimate control aim is to ensure the robust performance of the MSF plants at high thermal efficiency operating points under different constraints to lower the product costs and provide energy-efficient methods of purifying seawater.

2. MSF system description

2.1. Desalination process

MSF desalination is the evaporating and condensing processes, which are generally split into many stages. The MSF system includes three main sections: heat-rejection, heat-recovery and brine heater (Fig. 1). The heat-rejection and heat-recovery sections are the combinations of flashing chambers (stages) connected in series. Each stage consists of a brine pool, condenser tubes, a distillate tray, a demister and an orifice. Typically, the modern MSF plants with three stages in the heat-rejection section and 12–29 stages in the heat-recovery one will offer good performances [7]. The brine heater includes two separate streams, in which one stream is the recycle brine exiting from the first stage of the heat-recovery section, and the other stream is the low-pressure steam used to heat the first stream to the desired temperature.

In this model, intake cool seawater is first pumped into the condenser tubes of the heat-rejection section to get heated by the heat released from the condensation of flashing vapor in the chambers. A part of the stream leaving the heat-rejection section is rejected to the sea, and the other part will be mixed with the brine in the last stage of the heat-rejection section as make-up. The brine exiting from the final stage of heat-rejection section is partly recycled to the last stage of the heat-recovery section. For the flow to the first stage of the heat-recovery section, this recycle stream is gradually heated by the heat released from the condensation of flashing vapor in the chambers.

The pre-heated brine coming from the first stage of the heat-recovery section will be further heated to reach the required top brine temperature in the brine heater, and then it flows back into the heat-recovery section at the first stage.

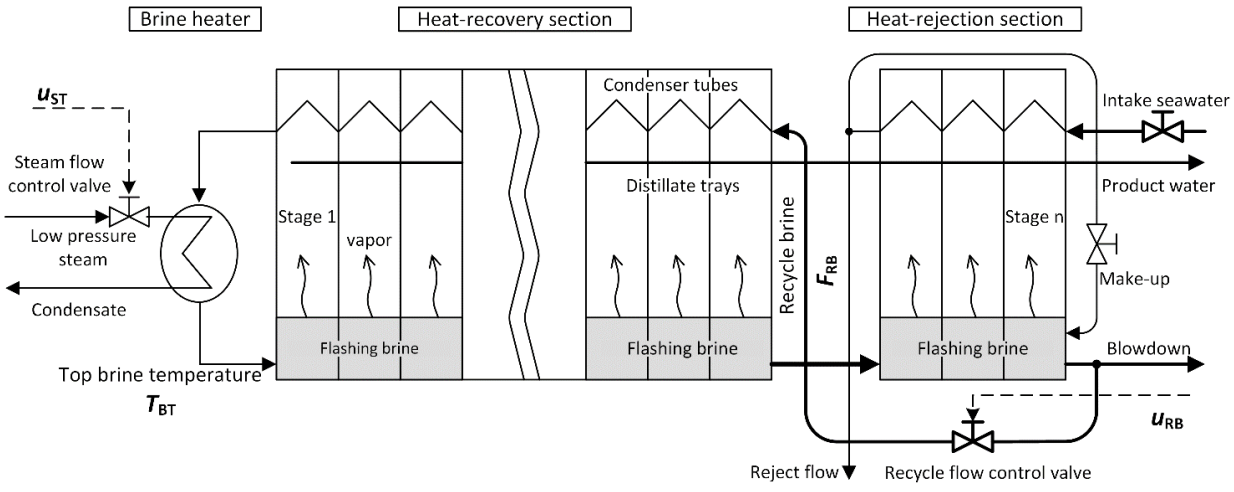

Fig. 1. A schematic diagram for circulating-brine MSF desalination plant.

This heated brine will be flashed off when moving through the stages with decreasing pressures. The flashing vapor will be condensed by the condenser tubes and collected from distillate trays as product water. One part of the concentrated brine coming out from the last stage of heat-rejection section is discharged as blow down, and the other will serve as mentioned recycle brine.

2.2. Physical model formulation

The design of an efficient controller requires a rigorous mathematical model of the MSF system. Several MSF process models have been proposed in the literature. They were formulated using some main methods such as tridiagonal matrix [8], state-by-state calculation [9], global methods [10], relaxation method [11] and combinations of methods [12]. Since MSF is a complicated and coupled nonlinear recycle process with closed-loop information flows, most of the dynamic models have been constructed using commercial software such as gPROMS [13], Aspen Plus [14], SPEEDUP [6,15,16], MATLAB [17] and IPSEpro [3].

In this paper, the system modeling is based on the physical equations in each unit; then they are coupled together to give the mathematical model for the complete desalination system. Each flash stage in MSF plant consists of four main components: the brine pool, distillation tray, vapor space and the condenser tubes as depicted in Fig. 2.

The modeling issue in this section is to show the relations between the system input and output variables. In order to reach the goal, top brine temperature (T_{BT}) and recycle brine flow (F_{RB}) are selected as controlled variables to represent the dynamic performance of a desalination process. In fact, they are the most influential controlled variables for monitoring MSF plants. In addition, the manipulate variables are steam-flow-control valve position (u_{ST}) and recycle-flow-control valve position (u_{RB}), respectively (see Fig. (1)). Some assumptions are made to simplify the modeling as follows:

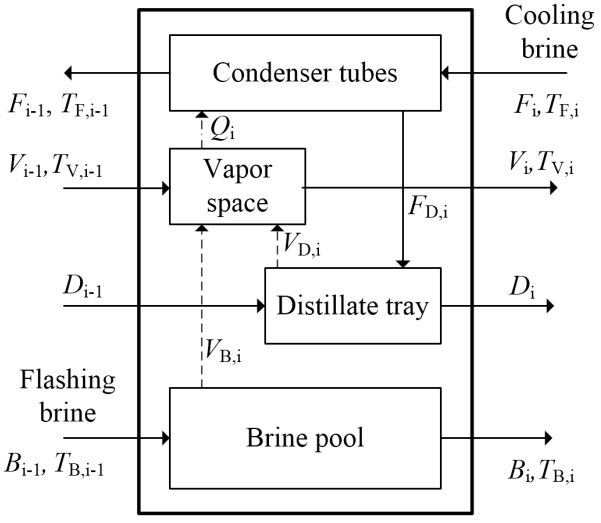

Fig. 2. Block diagram of the ith stage in the repeated stages.

- The brine is well mixed in every stage,
- The system is well insulated,
- No flashing occurs before entering the first flashing stage,
- The distillate temperature leaving any stage is the same as the vapor condensation temperature,
- The distillate product is salt-free,
- The effect of non-condensable gas and any holdup change for the cooling brine flowing inside the tubes is negligible.

Based on these assumptions and inherited from the dynamic model of Woldai et al. [15], the mathematical equations of an MSF plant with n stages are described below.

At first, the characteristics of recycle-flow-control valve give the relation between u_{RB} and F_{RB} as:

$$F_{RB} = F_{RB,max} R^{(u_{RB}-1)} \tag{1}$$

where $F_{RB,max}$ is the recycle brine flow at full opening, and R the range ability of the respective valve.

While u_{RB} relates to F_{RB} directly through Eq. (1), u_{ST} and T_{BT} have an indirect relation since the hot steam in brine heater and the recycle brine going out from condenser tubes in the first stages are separated streams. Note that this relation depends on the steam flow rate, recycle brine flow rate, and their temperatures. The steam flow rate is manipulated by steam-flow-control valve as follows:

$$F_{ST} = C_{vs} R^{(u_{ST}-1)} \sqrt{\Delta P} \tag{2}$$

where C_{vs} is the valve coefficient and ΔP the pressure drop through the valve.

The hot steam will heat the coming recycle brine in the brine heater to reach the top brine temperature $T_{BT.}$ Using the energy balance equation in the brine heater, this is described as follows:

$$M_{T,H} C_{F_{RB}} \frac{dT_{BT}}{dt} = F_{RB} C_{F_{RB}} (T_{F_{RB},1} - T_{BT}) + F_{ST}(H_{ST} - H_C) \tag{3}$$

where M is the mass hold up, C the heat capacity, F the flow rate and H the enthalpy; the subscript T indicates tubes, the subscript RB indicates recycle brine, the subscript ST indicates steam, and the subscript C indicates the condensate steam going out of brine heater.

In this model, only the distributed parameter is the brine temperature. In Eq. (3), $T_{FRB,1}$ is the brine temperature in condenser tubes of stage 1, which depends on the temperature and heat transfer of the other stages in the MSF process. The temperature T_{FRB} and heat transfer Q of any stage i, respectively expressed by the following equations:

$$M_{F_{RB}} C_{F_{RB}} \frac{dT_{F_{RB},i}}{dt} = F C_{F_{RB}} (T_{F_{RB},i-1} - T_{F_{RB},i}) + Q_i \tag{4}$$

and

$$Q_i = UA\Delta T_i \tag{5}$$

where U is the average heat transfer coefficient; A the condenser heat transfer area. Then ΔT can be calculated as follows:

$$\Delta T_{\mathrm{i}} = \frac{T_{\mathrm{F_{RB},i}} - T_{\mathrm{F_{RB},i\text{-}1}}}{\ln\left(\dfrac{T_{\mathrm{D,i}} - T_{\mathrm{F_{RB},i\text{-}1}}}{T_{\mathrm{D,i}} - T_{\mathrm{F_{RB},i}}}\right)} \tag{6}$$

The saturation temperature T_{D} is now given by:

$$T_{\mathrm{D,i}} = T_{\mathrm{B,i}} - T_{\mathrm{BPE}} - T_{\mathrm{NEA}} \tag{7}$$

where T_{BPE} is the total loss of temperature due to boiling point elevation and T_{NEA} is the non-equilibrium allowances. Next T_{B} is the temperature of flashing brine in the brine pool of any stage i given as follows:

$$M_{\mathrm{B,i}} C_{\mathrm{B,ave}} \frac{dT_{\mathrm{B,i}}}{dt} = B_{\mathrm{i-1}} H_{\mathrm{B,i-1}} - H_{\mathrm{B,i}}(B_{\mathrm{i-1}} - V_{\mathrm{B,i}}) - V_{\mathrm{B,i}} H_{\mathrm{V,B,i}} \tag{8}$$

where $C_{\mathrm{B,ave}}$ is the average heat capacitance of all brine pools, B the flashing brine flow rate and V the vapor flow rate in the brine pools.

In Eq. (8), the total mass balance in the brine pool and the vapor space are respectively, calculated as:

$$B_{\mathrm{i}} = B_{\mathrm{i-1}} - V_{\mathrm{B,i}} \tag{9}$$

$$V_{\mathrm{i}} + F_{\mathrm{D,i}} = V_{\mathrm{B,i}} + V_{\mathrm{D,i}} + V_{\mathrm{i-1}} \tag{10}$$

Then the condensation rate F_{D} is given by:

$$F_{\mathrm{D,i}} = \frac{Q_{\mathrm{i}}}{H_{\mathrm{V,i}} - H_{\mathrm{D,i}}} \tag{11}$$

where the subscript V indicates vapor and D implies distillation.

It is also noted that the last stage in the heat-rejection section receives the make-up flow F_{MK} while reject the recycle brine $F_{\mathrm{RB,max}}$ and the blowdown F_{BD}. Consequently, Eqs. (8) and (9) are modified as follows, respectively:

$$\begin{aligned} M_{\mathrm{B,n}} C_{\mathrm{B,ave}} \frac{dT_{\mathrm{B,n}}}{dt} &= B_{\mathrm{n-1}} H_{\mathrm{B,n-1}} + F_{\mathrm{MK}} H_{\mathrm{MK}} - H_{\mathrm{B,n}} \\ &\quad (B_{\mathrm{n-1}} + F_{\mathrm{MK}} - V_{\mathrm{B,n}}) - V_{\mathrm{B,n}} H_{\mathrm{V,B,n}} \end{aligned} \tag{12}$$

and

$$F_{\mathrm{RB,max}} = B_{\mathrm{n\text{-}1}} + F_{\mathrm{MK}} - V_{\mathrm{B,n}} - F_{\mathrm{BD}} \tag{13}$$

It can be seen that the dynamic relations between the inputs and outputs are represented by a set of differential equations and algebraic balances representing the dynamic model of any stage i and the brine heater. These dynamic models are complex with recycle flows and usually need computer-aided solvers to be further explored.

2.3. Controlled system model

Through the aforementioned MSF models, the fundamental parameters standing for dynamic performance are described by:

- Top brine temperature T_{BT},
- Recycle brine flow rate F_{RB},
- Low-pressure steam flow rate to the brine heater,
- Thermal performance ratio, which is the ratio of product water flow rate to the heating steam flow rate,
- Make-up seawater flow rate,
- Intake seawater flow rate,
- Intake seawater temperature,
- Brine level in the last stage of heat-rejection section.

The general control framework for the MSF process operations is constructed based on the interaction analysis of the manipulated and controlled variables. This is done by mean of the relative gain array (RGA). The analysis of RGA suggested some main pairings of manipulated and controlled variables for MSF process. They are identical in some studies as those of Woldai et al. [15] and Maniar and Deshpande [6], which include:

- Top brine temperature T_{BT} is controlled by the steam-flow-control valve position,
- Recycle brine flow rate F_{RB} is manipulated by the recycle-brine-flow-control valve position,
- Make-up flow rate is controlled by the make-up-flow-control valve position,
- Intake seawater flow rate is controlled by the intake-flow-control valve position.

Since T_{BT} and F_{RB} are the most influential controlled variables, they have been chosen to represent the dynamic performances of MSF process in this paper. Consequently, the manipulated variables are the steam-flow-control valve position u_{ST} and the recycle-brine-flow control valve position u_{RB}. In this study, the dynamic model has been estimated using empirical tools instead of mass, energy, and momentum balances. In fact the transfer function that relates the mentioned inputs and outputs of an 18-stage MSF plant was reported by Woldai et al. [15]. The second-order model with time-delay is given as follows:

$$G(s) = \begin{bmatrix} \dfrac{k_{11}(t_{n11}s+1)}{(t_{111}s+1)(t_{112}s+1)} & \dfrac{k_{12}(t_{n12}s+1)e^{-T_d s}}{(t_{121}s+1)(t_{122}s+1)} \\ 0 & k_{22} \end{bmatrix} \tag{14}$$

where k is the process gain, T_d time delay and t time constant. The transfer function relating to input/output vectors is given by:

$$Y(s) = G(s)U(s), \quad \text{with } U(s) = \begin{bmatrix} u_{\mathrm{ST}} \\ u_{\mathrm{RB}} \end{bmatrix}, \quad Y(s) = \begin{bmatrix} T_{\mathrm{BT}} \\ F_{\mathrm{RB}} \end{bmatrix} \tag{15}$$

For the transfer function in Eq. (14) to be expressed in rational polynomial form, the time-delay term can be described by the Pade approximation using second order:

$$e^{-T_d s} = \frac{1 - \dfrac{T_{\mathrm{d}}}{2}s + \dfrac{T_{\mathrm{d}}^2 s^2}{12}}{1 + \dfrac{T_{\mathrm{d}}}{2}s + \dfrac{T_{\mathrm{d}}^2 s^2}{12}} \tag{16}$$

From the system model in Eq. (14), it is noted that u_{RB} affects both F_{RB} and T_{BT} while u_{ST} only has effects on T_{BT}. Then T_{BT} and F_{RB} have direct effects on production and thermal efficiency. Increasing the F_{RB} will increase the total production but will decrease the performance ratio because more steam will be needed to heat the F_{RB} to the same as T_{BT} [14]. One major issue needed to be concerned is the scale formation inside the pipes. It is known that some of the main scaling factors are alkaline and non-alkaline scales such as $CaCO_3$ and $CaSO_4$ [18]. The scale formation strongly depends on temperature and pH in the process. If the brine is overheated, the high scale deposition will prevent the heat transfer and devastate system efficiency. On the other hand, the lower limit of F_{RB} is also fixed to avoid scaling caused by a low velocity of brine. Therefore, the T_{BT} and F_{RB} must be limited in their ranges to guarantee proper and safe operations for MSF plants. According to Al-shayji [19], the limits depend on the type of feed treatments. Typically, in the Persian gulf, the upper limit of T_{BT} at 110°C –112°C is set due to scaling problems and the lower limit is set at 90°C to avoid corrosion problems. The low velocity of brine will reduce heat-transfer coefficient and increase the sedimentation of solids on the heat-transfer surface. The lower limit of brine velocity is chosen at 1.8 m/s. Besides, the maximum flow rate for the recycle brine is limited by the maximum allowable velocity in the cooling tubes. The upper limit of brine velocity is set at 2 m/s to avoid erosion and carry-over of brine to the distillate.

The vital issue in the control problem of MSF plant, which is insufficiently considered in the literature, is the control robustness against uncertainty and disturbance. The uncertainties in the MSF desalination plants come from many sources during normal operations. For instance, some model parameters are poorly known, or they are variables due to changes in the operating conditions, such as the heat transfer coefficients in heating tubes are decreasing due to scaling; the temperature losing due to pressure drop through the tubes is also variable [20]. The presence of non-condensable gasses also causes large mismatches of brine density and vapor enthalpy. Besides the uncertainties, external disturbance and sensor noises should be considered in the actual MSF plant operations. In this paper, all the mentioned uncertainties are described by the parameter variations in the transfer function (Eq. (14)), as depicted in Table 1. The designed controller will be tested under a wide range of possible operating conditions of these model variations. It is expected to provide robust performance to overcome those uncertainties and have high ability of disturbance rejection and noise attenuation.

Table 1
The parameter variations in the MSF process model

Parameters	Min values	Nominal values	Max values
k_{11}	21.6	54	86.4
k_{21}	–131.2	–82	–32.8
k_{22}	216.4	541	865.6
t_{n11}	8.128	20.32	32.512
t_{n12}	9.952	24.88	39.808
t_{111}	7.32	18.3	29.28
t_{112}	2.88	7.2	11.52
t_{121}	3.432	8.58	13.728
t_{122}	3.384	8.46	13.536
T_d	0.012	0.03	0.048

3. The 2-DOF robust control synthesis

As mention above, the T_{BT} and F_{RB} have direct effects on the MSF performance, and they must be kept stable in their operation limits. In fact, there exist couplings between these variables. Besides, the system parameters in the MSF process are not fixed at their nominal values but do vary in their uncertainty ranges as described in Table 1. Furthermore, the control system copes with many external and unstable factors which can cause some unpredictable behaviors for controlled variables. As such a complex process, MSF plant requires an efficient and powerful control system to maintain its operations at optimal conditions that result in the low product costs and prevent system failures. In this section, a 2-DOF H_∞ loop-shaping controller is designed to bridge the gap between dynamic model and real desalination plant, and keep MSF plant stable, ensuring the desired performance even under high levels of disturbances and noises. Some concepts are firstly introduced before realizing the robust controller.

3.1. Coprime factor uncertainty of MSF system

The nominal process model in the MSF plant is described using the left coprime factorization (LCF) [21]:

$$G(s) = M(s)^{-1}N(s) \tag{17}$$

where $M(s), N(s) \in \Re H_\infty$ (i.e., proper and stable) are coprime factor matrices.

The uncertainty description of CFU is based on additive perturbations to the LCF. From the nominal system with no uncertainty in Eq. (17), two uncertainty blocks are added to form uncertain dynamical plant as depicted inside the dashed rectangle in Fig. 3. In this structure, the uncertainty blocks Δ enter and exit from the same position, and in turn they can be combined to form a full perturbation block. The CFU description is general and has distinct advantages over the other approaches that it is possible to represent a greater variety of the system uncertainty without prior information. This uncertainty captures both low and high-frequency perturbations in the model. Indeed, the uncertainty blocks Δ account for both unmodeled dynamics and physical parameter variations in the MSF system.

From the block diagram of CFU in Fig. 3, the real desalination system with uncertainty (or the perturbed system) is now expressed by:

$$G_p = (M_s + \Delta_M)^{-1}(N_s + \Delta_N),\ \left\| \begin{bmatrix} \Delta_N & -\Delta_M \end{bmatrix} \right\|_\infty \le \varepsilon = \gamma^{-1} \tag{18}$$

where ε is the stability margin and γ is the optimal cost, with M_s, N_s, Δ_M and $\Delta_N \in \Re H_\infty$.

According to small gain theorem, the closed-loop system will remain stable if:

$$\|\Delta\|_\infty = \left\| \begin{bmatrix} \Delta_N & -\Delta_M \end{bmatrix} \right\|_\infty \le \varepsilon \tag{19}$$

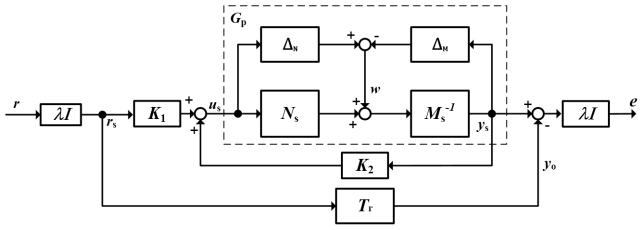

Fig. 3. 2-DOF control configuration with coprime factor uncertainty.

In turn, the stability margin ε can be calculated by:

$$\varepsilon = \left\{1 - \left\| N_s \;\; M_s \right\|_H^2 \right\}^{1/2} = (1 + \rho(XZ))^{-\frac{1}{2}} \tag{20}$$

where $\|\cdot\|_H$ denotes the Hankel norm and ρ denotes the spectral radius. For a minimal state-space realization (*A*, *B*, *C*, *D*) of the system, then *G*, *Z* and *X* are the unique positive definite solutions of the following algebraic Riccati equations:

$$\begin{aligned}&(A - BS^{-1}D^TC)Z + Z(A - BS^{-1}D^TC)^T \\ &\quad - ZC^TR^{-1}CZ + BS^{-1}B^T = 0\end{aligned} \tag{21}$$

$$\begin{aligned}&(A - BS^{-1}D^TC)^TX + X(A - BS^{-1}D^TC) \\ &-XBS^{-1}B^TX + C^TR^{-1}C = 0\end{aligned} \tag{22}$$

with $R = I + DD^T$ and $S = I + D^TD$.

It is noted that ε is the indicator of the robustness level of the complete control system. Various practical implementations show that ε > 0.25 is acceptable for robustness against uncertainty.

3.2. Loop-shaping technique

In the robust control paradigm, the control objective is to stabilize the set of perturbed plant G_p using a feedback controller *K* with a maximum amount of CFU (or the stability margin ε). Loop-shaping technique allows the system designer to specify closed-loop objectives by shaping the open-loop gains. Using two compensators W_1 and W_2 as depicted in Fig. 4, the original system *G*(s) is shaped by:

$$G_s(s) = W_2(s)G(s)W_1(s) = M_s^{-1}N_s \tag{23}$$

where W_2 is the identity matrix and W_1 is a diagonal matrix. In this setup they are used to shape the frequency response of the original MSF model and to specify the closed-loop behaviors.

Typically, the open-loop gains have to be large at low frequencies for good disturbance rejection at both input and output of the plant, and small at high frequencies for noise rejection. Besides, the desired open-loop shapes are chosen as approximately –20 dB/decade roll-off around the crossover frequency to realize desired robust stability and transient response.

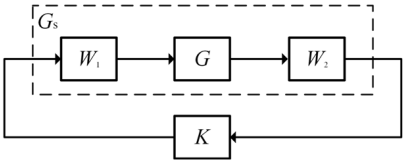

Fig. 4. Block diagram for the loop-shaping plant.

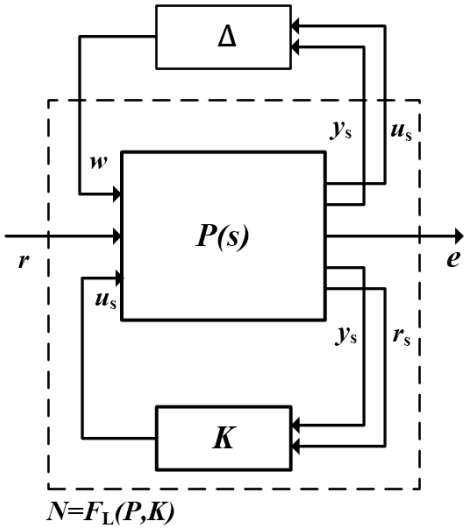

Fig. 5. General feedback interconnection for LFT setup.

3.3. The 2-DOF H_∞ loop-shaping controller for MSF system

In this paper, a dynamic 2-DOF controller has been proposed using the approach of Hoyle et al. [22] to satisfy both robustness and performance requirements. As depicted by the control scheme in Fig. 3, the 2-DOF controller includes the feedback part K_2 and the pre-compensator K_1. The former satisfies the requirements of internal and robust stability, disturbance rejection and measurement noise attenuation; and the latter optimizes the response of the overall system to the command input such that the output of the system would be close to that of a chosen ideal system T_r. The purpose of the pre-compensator K_1 is to ensure that:

$$\left\| T - T_r \right\|_\infty \le \gamma\lambda^{-2} \tag{24}$$

where the actual closed-loop transfer function between input and output is given as:

$$T = (I - G_sK_2)^{-1}G_sK_1 \tag{25}$$

and the parameter λ is used to weigh the relative importance of robust stability as compared with the model-matching in the design optimization.

Rearranging the control system shown in Fig. 3 leads to the general feedback control structure as illustrated in Fig. 5. There are three main components in this H_∞ control framework, in which *P(s)* is generalized plant, *K* denotes the 2-DOF controller, and $\Delta = [\Delta_N - \Delta_M]$ represents the uncertainty matrix.

According to Figs. 3 and 5, the generalized plant *P(s)* is further written as:

$$\begin{bmatrix} u_s \\ y_s \\ e \\ \hline r_s \\ y_s \end{bmatrix} = \underbrace{\left[\begin{array}{cc:c} 0 & 0 & I \\ M_s^{-1} & 0 & G_s \\ \lambda M_s^{-1} & -\lambda^2 T_r & \lambda G_s \\ \hdashline 0 & \lambda I & 0 \\ M_s^{-1} & 0 & G_s \end{array}\right]}_{P} \begin{bmatrix} w \\ r \\ \hline u_s \end{bmatrix} \tag{26}$$

where $w = \Delta \begin{bmatrix} u_s \\ y_s \end{bmatrix}$ and $u_s = K \begin{bmatrix} r_s \\ y_s \end{bmatrix}$.

The robustness criteria are based on small gain theory and μ-synthesis [21]. Therefore, it is necessary to connect the generalized plant *P(s)* with the controller *K* to create *N*-Δ structure so that μ-synthesis can be applied to this MSF plant. The control connection uses lower LFT, which is described by:

$$\begin{bmatrix} u_s \\ y_s \\ e \end{bmatrix} = F_L(P,K) \begin{bmatrix} w \\ r \end{bmatrix} \tag{27}$$

where

$$F_L(P,K) = N = \left[\begin{array}{c:c} K_2(I - G_s K_2)^{-1} M_s^{-1} & \lambda (I - K_2 G_s)^{-1} K_1 \\ (I - G_s K_2)^{-1} M_s^{-1} & \lambda (I - G_s K_2)^{-1} G_s K_1 \\ \hdashline \lambda (I - G_s K_2)^{-1} M_s^{-1} & \lambda^2 (I - G_s K_2)^{-1} G_s K_1 - T_r \end{array}\right] = \left[\begin{array}{c:c} N_{11} & N_{12} \\ \hdashline N_{21} & N_{22} \end{array}\right] \tag{28}$$

It is worth noting that the norm minimization of *N* may ensure both good model-matching and robust stability. The μ-synthesis with applying the small gain theorem leads to the condition that if $\|N_{11}\|_\infty \le \gamma$, then the closed-loop system will remain stable for all Δ such that $\|\Delta\|_\infty \le \gamma^{-1} = \varepsilon$. More specifically, according to Hoyle et al. [22] and Farlane and Glover [23], it turns out that the MSF is robustly stable if a controller is applied to satisfy the following condition:

$$\left\| \begin{bmatrix} K_2 \\ I \end{bmatrix} (I - G_s K_2)^{-1} M_s^{-1} \right\|_\infty \le \frac{1}{\varepsilon} \tag{29}$$

Then it is noted that K_2 can be calculated by:

$$K_2 = \left[\begin{array}{c|c} A + BF + \gamma^2 (L^T)^{-1} Z C^T (C + DF) & \gamma^2 (L^T)^{-1} Z C^T \\ \hline B^T X & -D^T \end{array}\right] \tag{30}$$

where

$$F = -S^{-1}(D^T C + B^T X) \tag{31}$$

$$L = (1 - \gamma^2) I + XZ \tag{32}$$

Finally, it turns out that the 2-DOF H_∞ loop-shaping controller for the perturbed plant G_p is derived as:

$$K = \begin{bmatrix} K_1 & W_1 K_2 W_2 \end{bmatrix} \tag{33}$$

3.4. Reduced-order controller

In general, the high-order controller is hard to be implemented practically, and it often causes time delays for the controlled system. Therefore, in this study, the synthesized controller with 15-orders is reduced to a valid low-order that achieves the equivalent levels of performance and robustness. By applying optimal Hankel norm approximation, a 6-order controller is attained that only has slight differences in the frequency and closed-loop time responses, comparing to the full-order controller. The further reduction of the controller order leads to severe deterioration of the closed-loop responses and would even cause the instability. Therefore, it is still safe to use the 6-order controller for the MSF process instead of the full-order controller.

4. Simulation setup

In this simulation, the mismatches between the MSF model and the real system are expressed by the parameter variations of the transfer function *G(s)* as shown in Table 1. Beside the set of parametric uncertainty, the system designers also introduce random disturbances at the system outputs and noise signals in the closed-loop system to verify controller's performance. The closed-loop system has been tested for robust stability and performance under given simulation conditions.

In the research of Woldai et al. [15], the parameters of PID controller need to be redesigned in six different operation conditions as summarized in Table 2. These operation points represent some different performance ratios. Therefore, they have to setup a parameter scheduling law so that the PID controller can run online. This kind of law is inconvenient, and the variations of controlled variables are obviously not fixed at some values. In this paper, the set-points for controlled variables are set using six conditions as proposed by Woldai et al. [15] for a better comparison. The controller should track new set-points without changing any control parameter.

For the sake of clarity, the system designers choose three models to represent the set of the perturbed system: the nominal model with nominal parameters, the minimum and maximum models with minimum and maximum parameters in Table 1, respectively.

The design criteria of the closed-loop system are selected as follows:

- The stability margin ε > 0.5.
- The effects of external disturbance and measurement noises are reduced at least 50%.

Table 2
Test conditions for control performance

Cases	T_{BT} (°C)	F_{RB} (*t*/*h*)
1	95	14,420
2	100	14,420
3	105	14,420
4	105	11,500
5	105	12,500
6	105	13,500

- The transient responses have settling times less than 1.5 min, less than 10% overshoot, and zero steady state errors.

The compensators W_1 and W_2 that enable the designer to achieve the desired loop shape in Eq. (23) are calculated as follows:

$$W_1(s)=\begin{bmatrix}\left[12\dfrac{s+0.4}{s+10^{-4}}\right]^2\left[\dfrac{4}{s+50}\right]^2 & 0\\ 0 & \left[\dfrac{1}{s}\right]\left[10\dfrac{s+0.03}{s+10^{-4}}\right]\left[\dfrac{3}{s+75}\right]^3\end{bmatrix} \tag{34}$$

$$W_2(s)=\begin{bmatrix}1 & 0\\ 0 & 1\end{bmatrix} \tag{35}$$

And the reference system is selected as:

$$T_r(s)=\begin{bmatrix}\dfrac{25}{s^2+7.07s+25} & 0\\ 0 & \dfrac{49}{s^2+14s+49}\end{bmatrix} \tag{36}$$

where the damping ratios (0.707 and 1, respectively) for the second-order responses have been chosen to meet the time-domain design criteria (e.g., rise time, maximum overshoot, settling time).

5. Test results and discussions

The frequency response (or singular value plot) is shown in Fig. 6 for the shaped loop and original model. It can be observed that the shaped loop has high gain at low frequency and low gain at high frequency as desired. These slopes are necessary to guarantee the disturbance and noise attenuations for the given frequency ranges. In the case of the original loop, the responses in the first channel will be deeply affected by disturbance because its slope is zero at low frequencies. The second channel will fluctuate in the same magnitude of disturbance and noise since there is no slope in its frequency response.

Based on the shaped loop, the 2-DOF H_∞ loop-shaping controller is synthesized using Eqs. (17)–(33). The achieved value of ε is 0.6 which indicates good stability gain and 60% of CFU is allowed. Thus, the designed controller can deal with parameters variations (Table 1) up to 60%.

The dynamic responses of the MSF system are divided into two channels: the first is from steam-flow-control valve position u_{ST} to top brine temperature T_{BT} and the second is from recycle-brine-flow-control valve position u_{RB} to recycle brine flow rate F_{RB}. Fig. 7 shows that the outputs can track new set-points of 6 different testing cases in a short rising time of less than 1 minute with slight overshoot in the first channel and no overshoot in the second. This result is imperative since high overshoots can bring the T_{BT} and F_{RB} out of safe zones and may cause fouling, erosion or certain faults. Furthermore, there is almost no difference between the

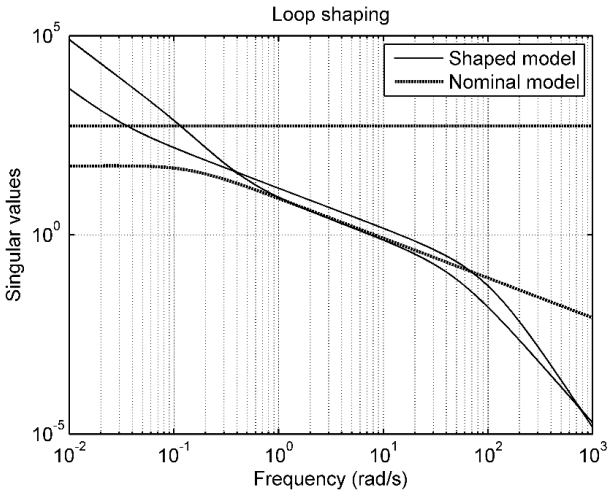

Fig. 6. Frequency responses for shaped loop and original loop.

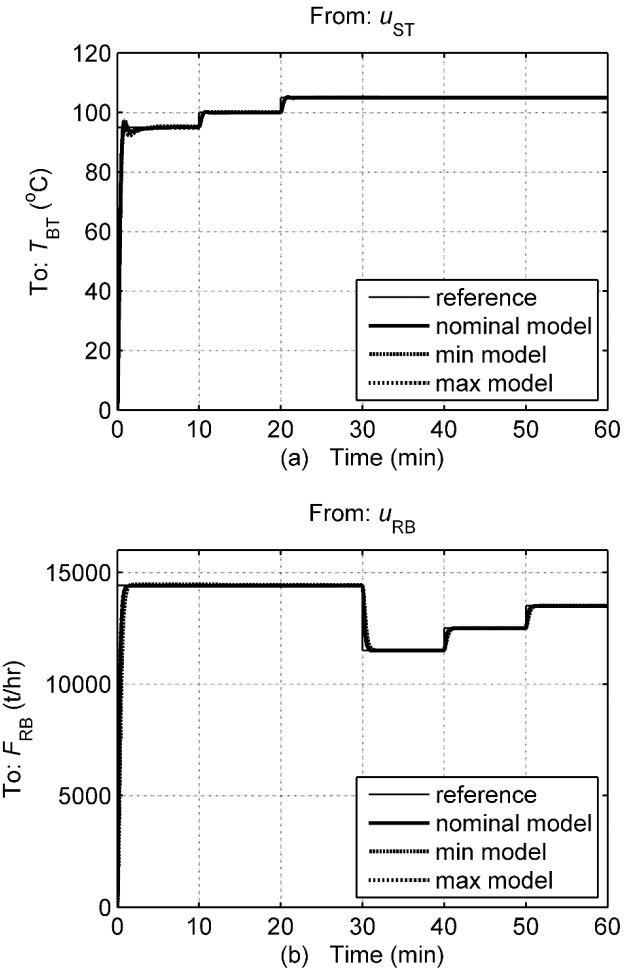

Fig. 7. Transient responses of the closed-loop system with 2-DOF H_∞ loop-shaping controller. (a) response in the first channel: from steam-flow-control valve position to top brine temperature; (b) response in the second channel: from recycle-brine-flow-control valve position to recycle brine flow.

responses of the nominal, minimum and maximum model. It proves that the achieved controller successfully overcomes the parameter uncertainties in MSF model plant, and it can keep the system in proper operation conditions. In comparison with other controllers such as PID controller presented by Chidambaram et al. [24] and MPC controller by Ali et al. [5], one can conclude that the proposed robust controller offers better performance on water quality even under severe uncertainties.

Figs. 8(a) and (b) shows the ability of disturbances attenuation for the robust controller. Recall that the disturbances can be the causes of biofouling, scale formation, actuator fault, changing in steam or feed temperature, feed water salinity, etc. In this study, the random disturbances have been applied in addition to reference inputs for real operations. As illustrated in those figures, the external disturbances are really attenuated. Specifically, a disturbance of 18 in magnitude starting at 20th min only causes a change of 2 in the T_{BT} and there are also very slight fluctuations in F_{RB}. It means at least 84% of disturbance is effectively eliminated. It is also worth to note that the fluctuations occur in a very short time. Along with this ability, the transient response without overshoot help to keep F_{RB} constant at some operation values and prevent carry-over of brine into the distillate or blow through the inter-stage orifices.

In practice, the external disturbances are often low-frequency signals, whereas the noises are often high-frequency signals. Noise is generally unavoidable and can cause some errors to the complete system. Therefore, it is crucial to eliminate noise effects on MSF plants for water monitoring. Input references with sensor noises have been applied into two channels. Figs. 8(c) and (d) shows the noise attenuation ability of the achieved controller at the high-frequency range. The time responses are scaled in ten minutes for better visualization. It can be observed that 90% of noises in the first channel and 80% in the second channel are successfully

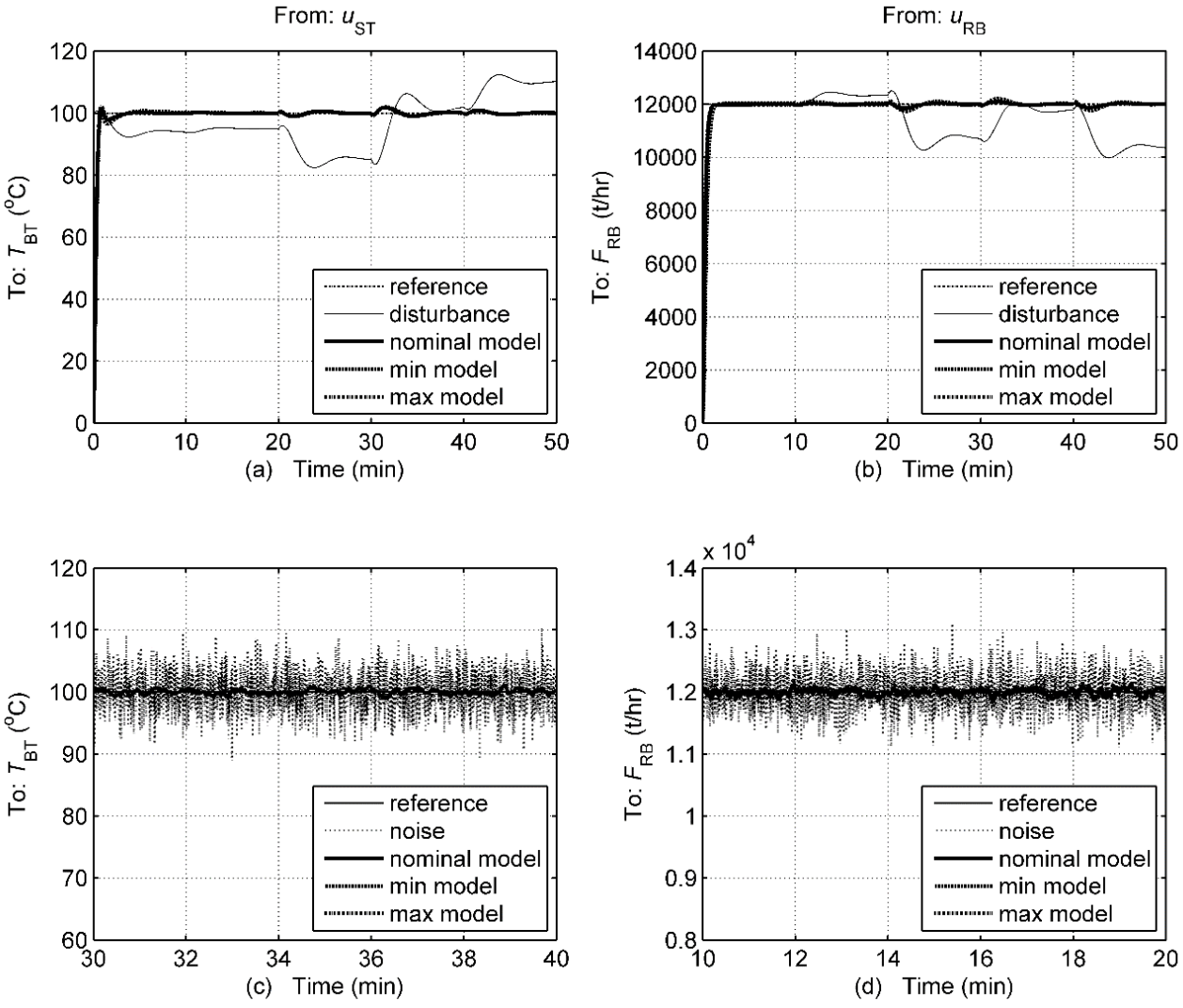

Fig. 8. System responses due to disturbances and noises with 2-DOF H_∞ loop-shaping controller. (a) disturbance response in the first channel; (b) disturbance response in the second channel; (c) noise response in the first channel; (d) noise response in the second channel.

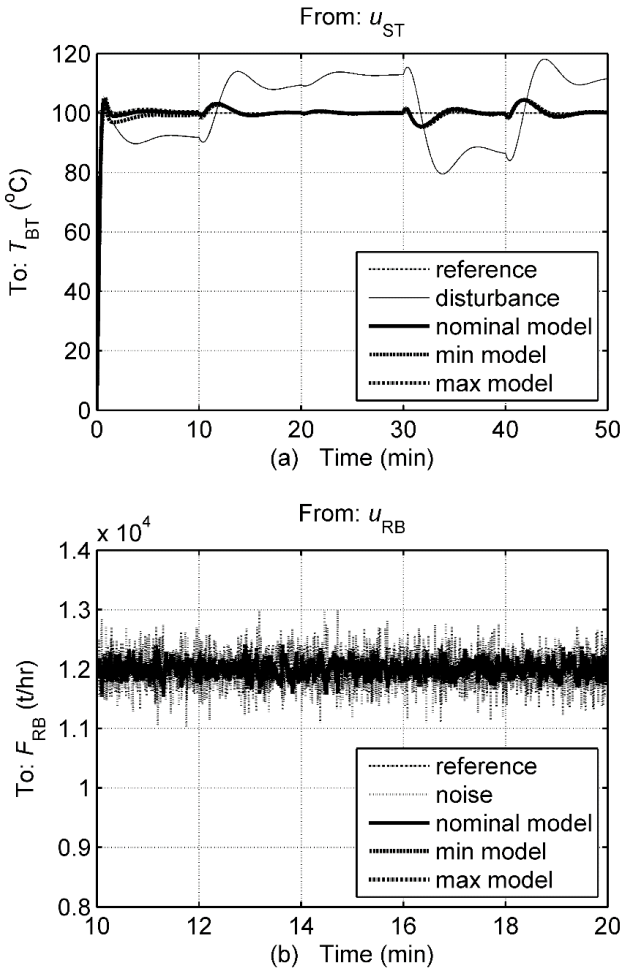

Fig. 9. The control performance of PID control scheme. (a) response due to disturbances in the first channel; (b) response due to noises in the second channel.

eliminated. From the magnitudes of noises and the changes in responses, one can conclude that the desalination system with the robust controller is unsusceptible to noises.

The performance of PID controller has been illustrated in Fig. 9 for comparison purposes. In Fig. 9(a), high overshoots and large differences between three models have been occurred in the first channel, under external disturbances. In the second channel, the F_{RB} is severely affected by noises (Fig. 9(b)). From these comparisons, it proves that the proposed robust controller is more effective than others reported in the desalination processes.

Finally, the proposed robust controller satisfies all the design requirements and demonstrates notable performances on the water qualities under the influence of unavoidable uncertainties, with overcoming the limitations of some conventional controllers.

6. Conclusions

The water desalination process is a highly complex dynamical system with some variables which are coupled and changing with time. Moreover, the parameter uncertainty, disturbance, and sensor noise make it difficult to control the MSF desalination plants at optimum conditions. In this paper, the 2-DOF H_∞ loop-shaping controller with reduced-order has been successfully designed to cope with these difficulties for MSF plant operations. By using CFU description, the parametric uncertainty can be modeled in a general form, which captures both unmodeled dynamics and physical parameter variations. Through the Hankel-norm approximation, the reduced 6-order control scheme offers computationally efficient algorithms for monitoring the MSF desalination plants. Simulation results show that the rise times of the controlled system are always less than 1 s. The robust controller can attenuate at least 84% of disturbances and 80% of noises, and deal with 60% of parameter variations, satisfying the performance requirements on water quality and energy consumption. In other words, the controller can keep the top brine temperature and recycle brine flow rate of MSF process to the desired values even under various uncertainties. When the controlled variables can be handled easily in their limits, the system designers can choose the performance ratio freely. This result also leads to robust design and operations for the MSF system by preventing of fouling and erosion as well as maintenance/repair free. Consequently, it will help increase water productivity and prolong the life of the desalination plants, guaranteeing energy-efficient method with lowering water product costs. Since the proposed controller has high robustness against uncertainties and disturbances, this method can be effectively used for monitoring the MSF desalination plants.

Abbreviations

CFU	—	Coprime factor uncertainty
DOF	—	Degree of freedom
LCF	—	Left coprime factorization
MPC	—	Model predictive controller
MSF	—	Multi-stage flash
PID	—	Proportional integral derivative

Symbols

A	—	Heat exchange area
B	—	Recycle brine flow rate
C	—	Specific heat capacity
D	—	Distillate flow rate
e	—	Scaled output
F	—	Flow rate in condenser tubes
F_L	—	Flow rate in condenser tubes
F_{RB}	—	Recycle brine flow rate
G	—	Nominal system
G_p	—	Perturbed plant
G_s	—	Shaped plant
H	—	Enthanpy
H_∞	—	Robust control
k	—	Process gain
K	—	Controller
M	—	Mass hold-up of Brine in water box
M_s, N_s	—	Normalized coprime factors
N	—	Controlled system
P	—	Generalized plant
Q	—	Heat

R — Reference input
S — Laplace variable
t — Time constant
T — Closed-loop transfer function, temperature
T_d — Time delay
T_r — Ideal system
T_{BT} — Top brine temperature
U — Internal energy, input
V — Vapor flow
W — Compensator
X — Concentration

Greek

γ — Optimal cost
ε — Stability gain margin
Δ_M, Δ_N — Uncertainty blocks
ρ — Spectral radius
λ — Scale factor

Subscripts

11 — From first input to first output
12 — From second input to first output
111 — First factor from first input to first output
112 — Second factor from first input to first output
121 — First factor from second input to first output
122 — Second factor from second input to first output
B — Brine
D — Distillate
F — Flow
H — Brine heater
in — Input
n — Numerator
out — Output
RB — Recycle brine
T — Tubes
V — Vapor

References

[1] J. Balraj, K. Pannerselvam, A. Jayaraman, Isolation of pigmented marine bacteria exiguobacterium Sp. From peninsular region of India and a study on biological activity of purified pigment, Int. J. Sci. Technol. Res., 3 375–384.
[2] I. Alatiqi, H. Ettouney, H. El-Dessouky, Process control in water desalination industry: overview, Desalination, 126 (1999) 15–32.
[3] F.N. Alasfour, K.H Abdulrahim, Rigorous steady state modeling of MSF-BR desalination system, Desal. Wat. Treat., 1 (2009) 259–276.
[4] M.A. Darwish, Ali Darwish, Amina Darwish, Fifty years of MSF desalination in Kuwait and sustainability issues, Desal. Wat. Treat., 29 (2011) 343–354.
[5] E. Ali, K. Alhumaizi, A. Ajbar, Robust control of industrial multi stage flash desalination plants, Desalination, 114 (1997) 289–302.
[6] V.M. Maniar, P.B. Deshpande, Advanced controls for multi-stage flash (MSF) desalination plant optimization, J. Proc. Cont., 6 (1996) 49–66.
[7] H. EI-Dessouky, I. Alatiqi, H. Ettouney, Process synthesis: the multi-stage flash desalination system, Desalination, 115 (1998) 155–179.
[8] A.M. Helal, M.S. Medani, M.A. Soliman, A tridiagonal matrix model for multistage flash desalination plants, Comput. Chem. Eng., 10 (1986) 327–342.
[9] W.K. Lewis, G.L. Matheson, studies in distillation, Ind. Eng. Chem., 24 (1932) 494–498.
[10] C.G. Broyden, A class of methods for solving nonlinear simultaneous equations, Math. Comp., 19 (1965) 577–593.
[11] A. Rose, R.F. Sweeney, V.N. Schrodt, Continuous distillation calculations by relaxation method, Ind. Eng. Chem., 50 (1958) 737–742.
[12] R.G. Ketchum, A combined relaxation-Newton method as a new global approach to the computation of thermal separation processes, Chem. Eng. Sci., 34 (1979) 387–397.
[13] H. Al-Fulaij, A. Cipollina, H. Ettouney, D. Bogle, Simulation of stability and dynamics of multistage flash desalination, Desalination, 281 (2011) 404–412.
[14] W. Lian-ying, X. Sheng-nan, G. Cong-jie, Simulation of multi-stage flash desalination process, Adv. Mater. Phys. Chem., 2 (2012) 200–205.
[15] A. Woldai, D.M.K. Al-Gobaisi, R.W. Dunn, G.P. Rao, Simulation aided design and development of an adaptive scheme with optimally tuned PID controller for a large multistage flash seawater desalination plant-Part I, II, III, Contr. Appl., (1995) 835–841.
[16] A. Hussain, A. Woldai, A. Al-Radif, A. Kesou, R. Borsani, H. Sultan, P.B. Deshpandey, Modelling and simulation of a multi-stage flash desalination plant, Desalination, 97 (1994) 555–586.
[17] M.B. Ali, L. Kairouani, Solving equations describing the steady-state model of MSF desalination process using Solver Optimization Tool of MATLAB software, Desal. Wat. Treat., 52 (2014) 7473–7483.
[18] A.E. Al-Rawajfeh, S. Ihm, H. Varshney, A.N. Mabrouk, Scale formation model for high top brine temperature multi-stage flash (MSF) desalination plants, Desalination, 350 (2014) 53–60.
[19] K.A. Al-Shayji, Modeling, Simulation and Optimization of Large Scale Commercial Desalination Plants, Doctor Dissertation Submitted to the Faculty of the Virginia Polytechnic Institute and State University, Blacksburg, Virginia, 1998.
[20] E. Ali, K. Alhumaizi, A. Ajbar, Model reduction and robust control of multi-stage flash desalination plants, Desalination, 121 (1999) 65–85.
[21] J. Doyle, Analysis feedback systems with structured uncertainties, IEE Proc. Control Theory Appl., 129 (1982) 242–250.
[22] D.J. Hoyle, R.A. Hyde, D.J.N. Limebeer, An H_∞ approach to two degree of freedom design, Proc. IEEE Conf. Decision Contr., Brighton, England, 1991, pp. 1581–1585.
[23] M. Farlane, D. Glover, Loop-shaping design procedure using H_∞ synthesis, IEEE Trans. Autom. Control, 37 (1992) 759–765.
[24] M. Chidambaram, B.C. Reddy, D.M.K. Al-Gobaisi, Design of robust SISO PI controllers for an MSF desalination plant, Desalination, 109 (1997) 109–119.